Supplementary Fig. 1

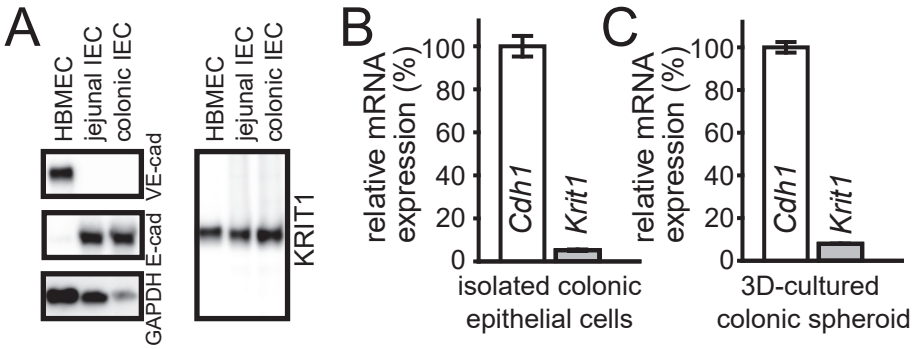

Supplementary Figure 1. KRIT1 is expressed in mouse intestinal epithelium.
A. Western blot of KRIT1 in isolated mouse jejunal and colonic epithelial cells. HBMEC cells was used as positive control. B-C. Quantitative RT-PCR of KRIT1 on isolated colonic epithelial cells (B) and 3D cultured colonic spheroids (C). *Cdh1* (E-cadherin) was used as positive control.

Supplementary Fig. 2

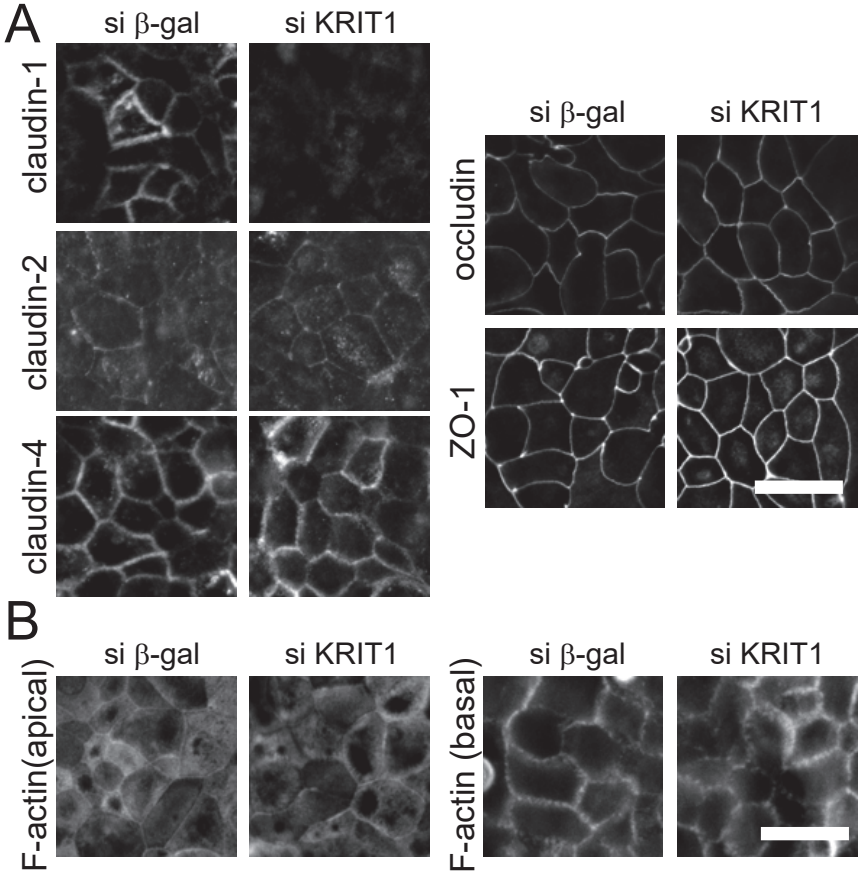

Supplementary Figure 2. Apical junctional component expression and localization in KRIT1 knockdown cells.
Immunofluorescent microscopy of tight junction proteins (A) and actin cytoskeleton (B) in control and KRIT1 knockdown monolayers. Bar=10 μm.

Supplementary Fig. 3

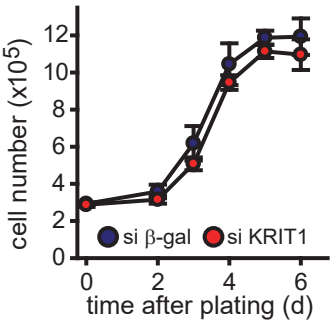

Supplementary Figure 3. Control and KRIT1 knockdown cells grow similarly.
Control and KRIT1 knockdown cells were plated at $3x10^5$ cell per well and cell number at indicated days post plating were quantified. Data are from four independent experiments.

Supplementary Fig. 4

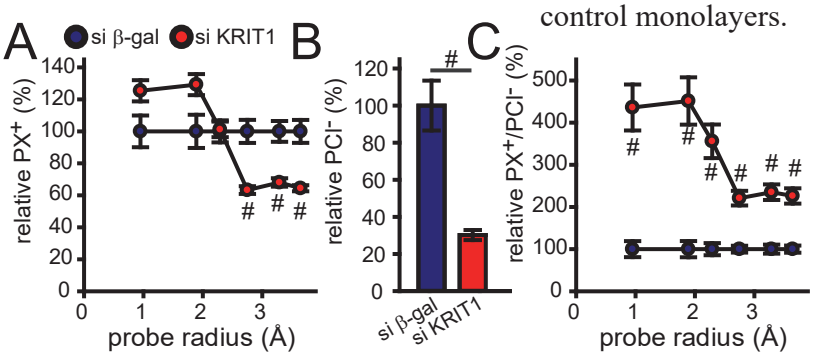

Supplementary Figure 4. KRIT1 knockdown decreases large cation and Cl^- permeability.
Permeability data presented in Fig. 2D-F are normalized to control monolayers, to demonstrate relative change between control (blue circles) and KRIT1 knockdown cells (red circles). A. Relative permeability of different sized monovalent cations, normalized to each cation in control monolayers. B. Relative permeability of Cl^-, normalized to control monolayers, F. Relative permeability of different sized monovalent cations to Cl^-, normalized to each cation in control monolayers.

Supplementary Fig. 5

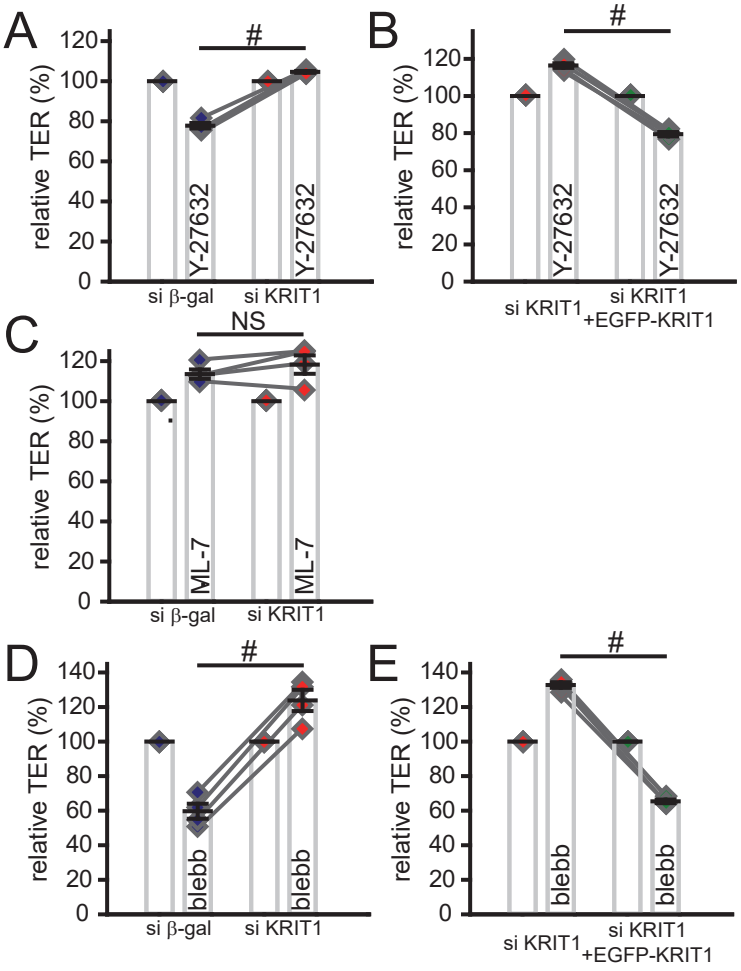

Supplementary Figure 5. KRIT1 knockdown limits ROCK- and myosin II motor- inhibition induced barrier dysfunction.
TER data from Fig. 3A-C and Fig. 4C-D are normalized to demonstrate relative changes of each cell line following treatment. A. Relative TER of ROCK inhibitor Y-27632 (20 μM) treated control (blue diamonds) and KRIT1 knockdown (red diamonds) monolayers. Data points from same individual experiments are connected by gray lines. B. Relative TER of Y-27632 (20 μM) treated KRIT1 knockdown cells stably transfected with Tet-inducible EGFP-KRIT1 plasmid with (green diamonds) or without (red diamonds) doxycycline induced EGFP-KRIT1 expression, normalized to each condition. Data points from same individual experiments are connected by gray lines. C. Relative TER of MLCK inhibitor ML-7 (20 μM) treated control (blue diamonds) and KRIT1 knockdown (red diamonds) monolayers, normalized to each cell line. Data points from same individual experiments are connected by gray lines. D. Relative TER of myosin II motor inhibitor blebbistatin (50 μM) treated control (blue diamonds) and KRIT1 knockdown (red diamonds) monolayers, normalized to each cell line. Data points from same individual experiments are connected by gray lines. E. Relative TER of blebbistatin (50 μM) treated KRIT1 knockdown cells stably transfected with Tet-inducible EGFP-KRIT1 plasmid with (green diamonds) or without (red diamonds) doxycycline induced EGFP-KRIT1 expression, normalized to each condition. Data points from same individual experiments are connected by gray lines.

Supplementary Fig. 6

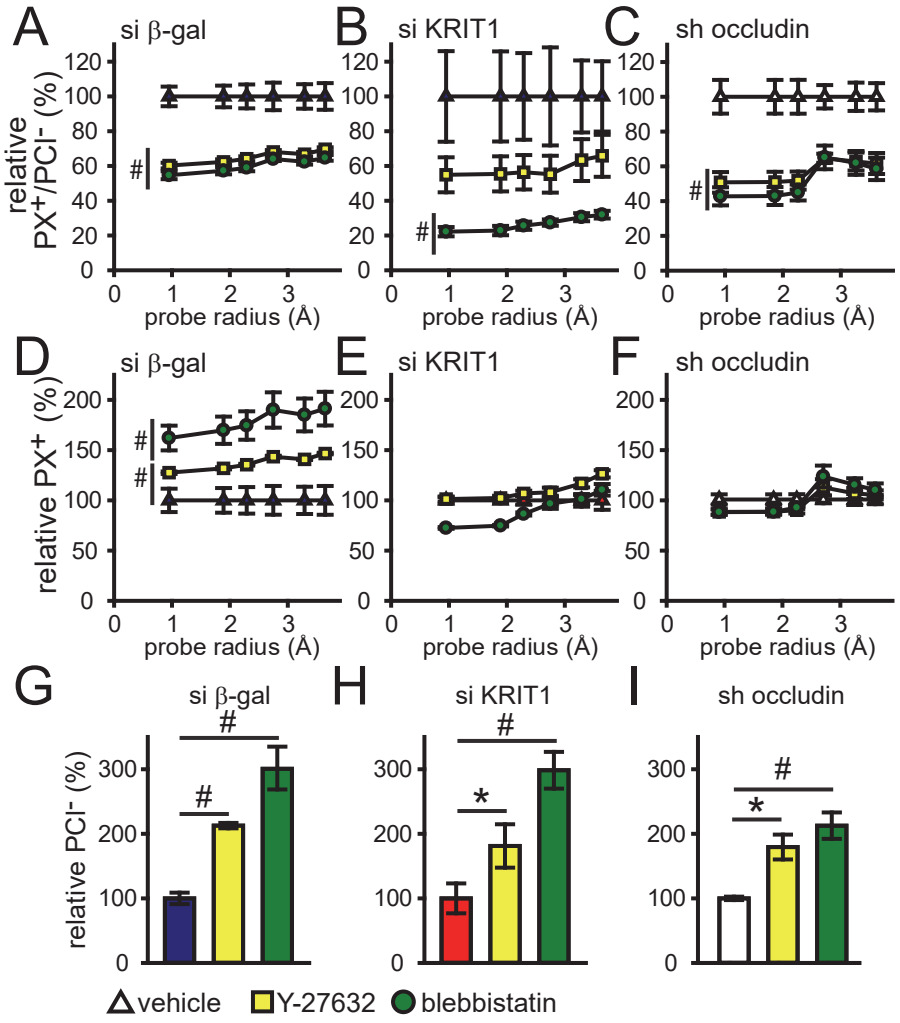

Supplementary Figure 6. ROCK-Myosin II motor-dependent regulation of tight junction "leak" pathway requires KRIT1 and occludin.
Permeability data from Fig. 5A-I are normalized to vehicle treated monolayers of each cell lines used, to demonstrate relative changes within each cell line following treatment. A-C. Relative permeability of different sized cations to Cl^- of Y-27632 (20 μM, yellow squares) or blebbistatin (50 μM, green circles) treated control (A, blue triangles), KRIT1 knockdown (B, red triangles), and occludin knockdown (C. white triangles) monolayers, normalized to each cation in each cell line. D-F. Relative permeability of different sized cations of Y-27632 (20 μM, yellow squares) or blebbistatin (50 μM, green circles) treated control (D, blue triangles), KRIT1 knockdown (E, red triangles), and occludin knockdown (F. white triangles) monolayers, normalized to each cation in each cell line. G-I. Relative permeability of Cl^- in Y-27632 (20 μM, yellow bars) or blebbistatin (50 μM, green bars) treated control (G, blue bar), KRIT1 knockdown (H, red bar), and occludin knockdown (I, white bar) monolayers, normalized to each cation in each cell line.

Supplementary Fig. 7

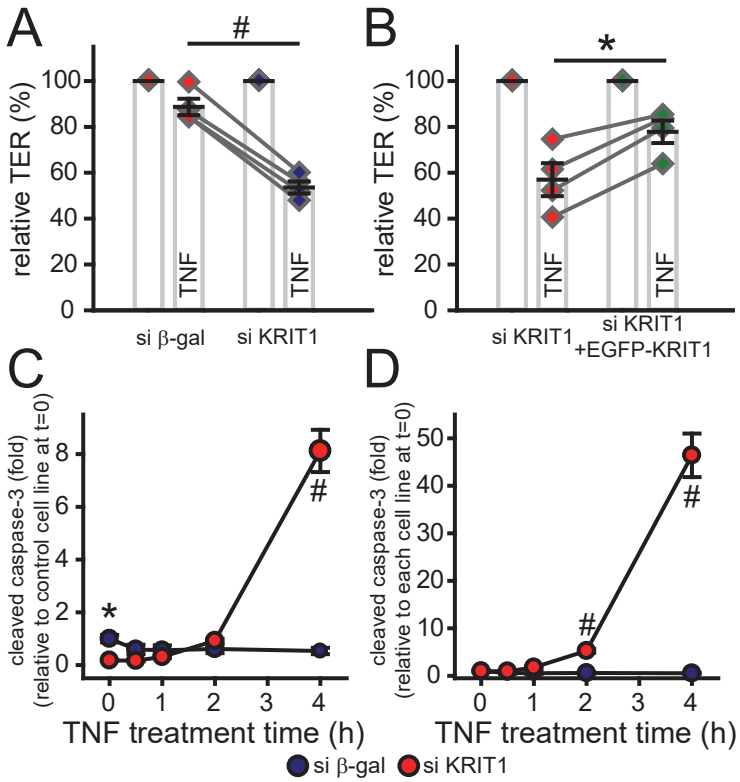

Supplementary Figure 7. KRIT1 limits TNF-induced epithelial barrier loss.
A-B. TER data from Fig. 6A-B are normalized to demonstrate relative changes of each cell line following treatment. A. Relative TER of TNF treated control (blue diamonds) and KRIT1 knockdown (red diamonds) monolayers, normalized to each cell line. All monolayers were pretreated with IFNγ 16-24 h to induce TNF receptor expression. Data points from same individual experiments are connected by gray lines. B. Relative TER of TNF treated KRIT1 knockdown cells stably transfected with Tet-inducible EGFP-KRIT1 plasmid with (green diamonds) or without (red diamonds) doxycycline induced EGFP-KRIT1 expression, normalized to each condition. All monolayers were pretreated with IFNγ 16-24 h to induce TNF receptor expression. Data points from same individual experiments are connected by gray lines. C-D. Quantification of cleaved caspase-3 band intensity, normalized to average of normalized GAPDH and E-cadherin band intensity. Data were either normalized to control monolayers not treated with TNF (C), or monolayers of each cell line not treated with TNF (D). Data was from three independent experiments.

Supplementary Fig. 8

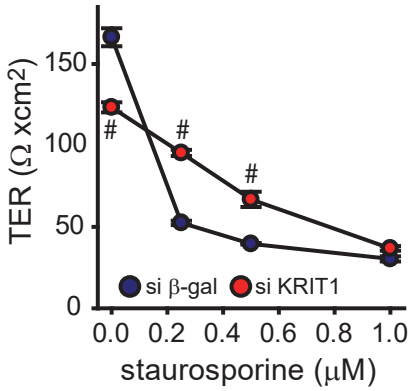

Supplementary Figure 8. KRIT1 knockdown cells are less sensitive to staurosporine induced barrier loss.
TER of control (blue circle) and KRIT1 knockdown (red circle) monolayers treated with different concentrations of pan-protein kinase inhibitor staurosporine.

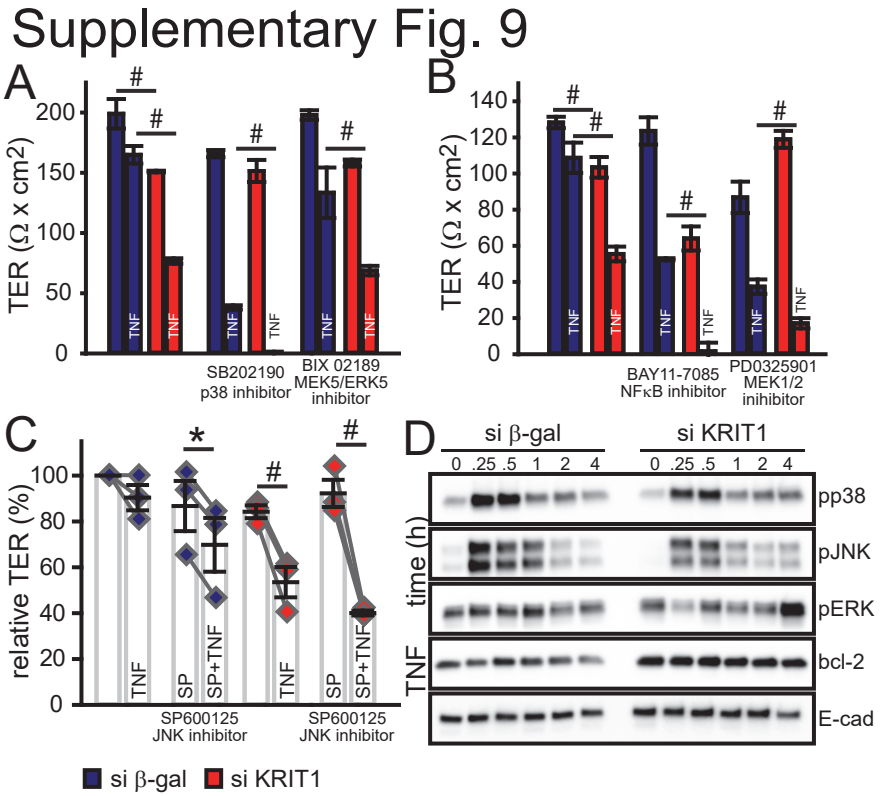

Supplementary Figure 9. KRIT1 loss exacerbated TNF-induced epithelial barrier dysfunction cannot be reversed by inhibitors of kinases that participate in TNF signaling.
A-C. TER of p38 inhibitor SB202190 (A), MEK5/ERK5 inhibitor BIX 02189 (A), NF_KB inhibitor BAY11-7085 (B), MEK1/2 inhibitor PD0325901 (B), as well as JNK inhibitor SP600125 (C) treated control (blue bars) and KRIT1 knockdown (red bars) monolayers with or without TNF (7.5 ng/ml) treatment. All monolayers were pretreated with IFNγ 16-24 h to induce TNF receptor expression. D. Western blot of phosphorylated kinases and bcl-2 in control and KRIT1 knockdown monolayers. All monolayers were pretreated with IFNγ 16-24 h to induce TNF receptor expression.

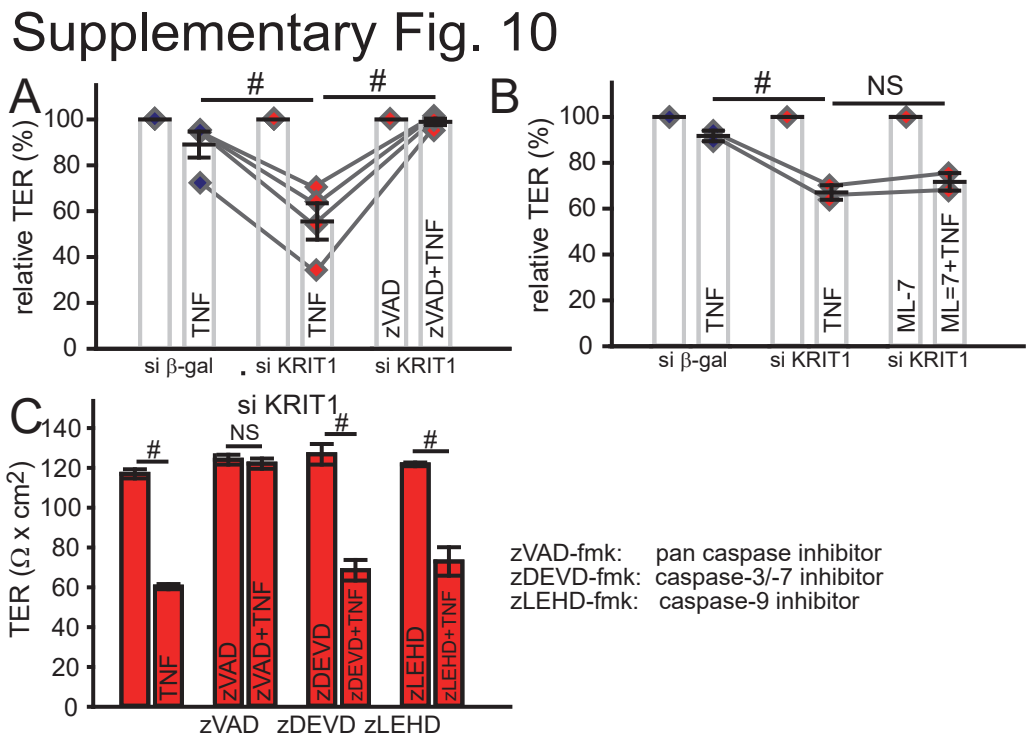

Supplementary Figure 10. KRIT1 loss exacerbates TNF-induced barrier dysfunction through enhancing apoptosis.
A-B. Relative TER of TNF (7.5 ng/ml) treated monolayers in the presence of pan-caspase inhibitor zVAD-fmk (A, 50 μM, four independent experiments) or MLCK inhibitor ML-7 (B, 20 μM, two independent experiments), normalized to control of each pretreatment condition. All monolayers were pretreated with IFNγ 16-24 h to induce TNF receptor expression. Data points from same individual experiments are connected by gray lines. C. TER of vehicle treated, pan-caspase inhibitor zVAD-fmk, caspase-3/-7 inhibitor zDEVD-fmk and caspase-9 inhibitor zLEHD treated KRIT1 knockdown monolayers with or without TNF (7.5 ng/ml) treatment. All monolayers were pretreated with IFNγ 16-24 h to induce TNF receptor expression.